Novel Venom Proteins Produced by Differential Domain-Expression Strategies in Beaded Lizards and Gila Monsters (genus *Heloderma*)

Bryan G. Fry,*[,1] Kim Roelants,[1,2] Kelly Winter,[3] Wayne C. Hodgson,[3] Laura Griesman,[1,3] Hang Fai Kwok,[4] Denis Scanlon,[5] John Karas,[5] Chris Shaw,[4] Lily Wong,[3] and Janette A. Norman[1,6]

[1]Venomics Research Laboratory, Department of Biochemistry and Molecular Biology, Bio21 Molecular Science and Biotechnology Institute, University of Melbourne, Parkville, Victoria, Australia

[2]Unit of Ecology and Systematics, Vrije Universiteit Brussel, Pleinlaan 2, Brussels, Belgium

[3]Monash Venom Group, Department of Pharmacology, Monash University, Clayton, Victoria, Australia

[4]Molecular Therapeutics Research, School of Pharmacy, Queen's University, Belfast, Northern Ireland, United Kingdom

[5]Bio21 Molecular Science and Biotechnology Institute, University of Melbourne, Parkville, Victoria, Australia

[6]Sciences Department, Museum Victoria, G.P.O. Box 666, Melbourne, Victoria, Australia

***Corresponding author:** E-mail: bgf@unimelb.edu.au.

Associate editor: Scott Edwards

Research article

Abstract

The origin and evolution of venom proteins in helodermatid lizards were investigated by multidisciplinary techniques. Our analyses elucidated novel toxin types resultant from three unique domain-expression processes: 1) The first full-length sequences of lethal toxin isoforms (helofensins) revealed this toxin type to be constructed by an ancestral monodomain, monoproduct gene (beta-defensin) that underwent three tandem domain duplications to encode a tetradomain, monoproduct with a possible novel protein fold; 2) an ancestral monodomain gene (encoding a natriuretic peptide) was medially extended to become a pentadomain, pentaproduct through the additional encoding of four tandemly repeated proline-rich peptides (helokinestatins), with the five discrete peptides liberated from each other by posttranslational proteolysis; and 3) an ancestral multidomain, multiproduct gene belonging to the vasoactive intestinal peptide (VIP)/glucagon family being mutated to encode for a monodomain, monoproduct (exendins) followed by duplication and diversification into two variant classes (exendins 1 and 2 and exendins 3 and 4). Bioactivity characterization of exendin and helokinestatin elucidated variable cardioactivity between isoforms within each class. These results highlight the importance of utilizing evolutionary-based search strategies for biodiscovery and the virtually unexplored potential of lizard venoms in drug design and discovery.

Key words: venom, adaptive evolution, molecular evolution, protein, toxin, Heloderma, byetta, exendin.

Introduction

Despite a state of fame that extends far beyond the fields of herpetology and natural history, *Heloderma suspectum* ssp (Gila Monsters) and *Heloderma horridum* ssp Mexican (beaded lizards) have remained remarkably enigmatic animals. Due to their secretive ecology and persistent folkloristic misconceptions that strongly influenced earlier scientific reports (Brown and Carmony 1999; Beck 2005), clinical and evolutionary aspects regarding the venom system of *Heloderma* lizard have long remained controversial. Ambiguities regarding individual toxin types persist even today. For example, the therapeutically useful exendin peptides have been referred to as originating from the "saliva" (Bloomgren et al. 2008). However, they have in fact only ever been isolated from venom (Parker et al. 1984; Eng et al. 1990, 1992), and mRNA coding for these toxins have only been recovered from venom glands (Chen and Drucker 1997; Chen et al. 2002, 2006).

Helodermatid lizard venoms are produced by compartmentalized glands on the lower jaw. Recent studies have shown that these glands share an ancient homology with those of other taxa within the reptile clade Toxicofera, which includes snakes and several other lizards recently shown to be venomous (Vidal and Hedges 2005; Fry et al. 2006). In contrast to the hypothesis of independent venom origins, this new perspective reveals that *Heloderma* and snake venom systems are homologous, but highly differentiated, descendants of an early evolved venom system in squamates that possessed incipient glands in both the mandibular and maxillary regions. Although snakes subsequently underwent further specialization of the maxillary venom glands and secondarily lost the mandibular ones, the anguimorph lizards (which include helodermatids and varanids) underwent the opposite trend, resulting in specialized mandibular glands (Fry et al. 2006). Although the *Heloderma* venom delivery system seems less sophisticated than the high-pressure injection mechanism of the front-fanged advanced snakes, the effect of *Heloderma* venom may be as clinically complex (Bogert and del Campo 1956; Bouabboud and Kardassakis 1988; Hooker and Caravati 1994; Strimple

Table 1. Helodermatid Venom Proteins and Characterized Activities.

Toxin Type	Species	Accession Numbers/References	Toxic Bioactivity
CRISP	*Heloderma horridum horridum*	Q91055 (Mochcamorales et al. 1990; Morrissette et al. 1995; Nobile et al. 1994, 1996)	Blockage of ryanodine receptors and potassium channels producing lethargy, paralysis, and hypothermia
Exendin 1	*Heloderma suspectum*ssp	P04203 (Parker et al. 1984)	Induction of hypotension-mediated by relaxation of cardiac smooth muscle (Grundemar and Hakanson 1992; Uddman et al. 1999; Tsueshita et al. 2004) and this study
Exendin 2	*H. suspectum* ssp, *Heloderma suspectum cinctum*	P04204 (Parker et al. 1984); This study: EU790960	Induction of hypotension mediated by relaxation of cardiac smooth muscle (Grundemar and Hakanson 1992; Uddman et al. 1999; Tsueshita et al. 2004) and this study
Exendin 3	*H. h. horridum*, *H. s. suspectum*	P20394 (Eng et al. 1990; Chen et al. 2006)	Induction of hypotension mediated by relaxation of cardiac smooth muscle (this study)
Exendin 4	*H. h. horridum*, *H. s. suspectum*, *H. s. cinctum*	P26349 (Eng et al. 1992; Chen and Drucker 1997; Neidigh et al. 2001; Chen et al. 2006); This study: EU790959	Induction of hypotension mediated by relaxation of cardiac smooth muscle (this study)
Helofesins	*H. h. horridum*, *H. s. cinctum*	Q7LZ31 (Komori et al. 1988); This study: EU790964, GQ918270, and GQ918271	Lethal inhibition of direct electrical stimulation
Helokinestatin-1	*H. h. horridum*, *H. s. suspectum*	(Kwok et al. 2008); this study	Bradykinin inhibition (Kwok et al. 2008) and this study
Helokinestatin-2	*H. s. cinctum*	This study: EU790965	Bradykinin inhibition (this study)
Helokinestatin-3	*H. s. cinctum*	This study: EU790965	Bradykinin inhibition (this study)
Helokinestatin-4	*H. s. cinctum*	This study: EU790965	Bradykinin inhibition (this study)
Kallikrein	*H. h. horridum*	P43685 (Mebs 1969a, 1969b; Nikai et al. 1988; Utaisincharoen et al. 1993)	Release of bradykinin from kinogen; a derived form cleaves fibrinogen
Natriuretic peptide	*H. s. cinctum*	This study: EU790965	Potent induction of hypotension leading to loss of consciousness; mediated through the binding of GC-A resulting in the relaxation of cardiac smooth muscle (this study)

et al. 1997; Cantrell 2003) with symptoms of *Heloderma* envenomation including extreme pain, acute local swelling, nausea, fever, faintness, myocardial infarction, tachycardia, hypotension, and inhibition of blood coagulation.

Reptile venom proteins are the result of the duplication of an ordinary body protein, often one involved in a key physiological process, with the subsequent tissue-specific expression of the new gene (Fry et al. 2005). It has been previously demonstrated that a core set of venom genes evolved in the common ancestor of the Toxicofera (Fry et al. 2006). Additional toxin recruitment events facilitated the development into the more complex venoms observed in extant snakes and lizards (cf. Fry et al. 2008). Currently, six protein-scaffold families have been identified in *Heloderma* venom (table 1). Two of these (CRISP and kallikrein) are homologous to proteins found in snake and other venoms, whereas the others are either shared with varanid lizard venoms (type III phospholipase A_2) or currently known only from *Heloderma* venoms (exendin and lethal toxin). Functionally important toxin types are reinforced through adaptive evolution involving explosive duplication and diversification, creating a venom gland specific multigene family. The likelihood for neofunctionalization is increased through random mutation, gene conversion, and unequal crossing-over (Fry et al. 2003). Although the molecular scaffold of the ancestral protein is conserved, derived activities emerge through mutations of the surface chemistry (de la Vega et al. 2003; Fry et al. 2003; Mouhat et al. 2004; Fry 2005).

In addition to evolutionary tinkering of ancestral molecular scaffolds, toxin diversity has been shown to be obtained in snake venoms through much more fundamental processes. This is characterized either by selective expression of a monodomain from an ancestral multidomain-encoding gene through exon deletion or a newly multidomain, multiproduct encoding gene evolving from a monoproduct, monodomain gene (fig. 1). The multidomain, multiproduct encoding SVMP (snake venom metalloprotease) gene (cf., Fox and Serrano 2008, 2009) is a particularly fascinating example of the former as two variants of selective domain expression having been independently derived: the propeptide domain in P-III type SVMP selectively expressed in *Psammophis mossambicus* venom with newly evolved cysteine bonds (fig. 1*A*) (Fry et al. 2008); and the P-II SVMP disintegrin domain selectively expressed in Viperidae venoms (fig. 1*B*) (cf. Calvete et al. 2005). An example of a multidomain, multiproduct gene evolving from a monodomain, monoproduct gene is the sarafotoxin type from *Atractaspis* venom (cf. Takasaki et al. 1988;

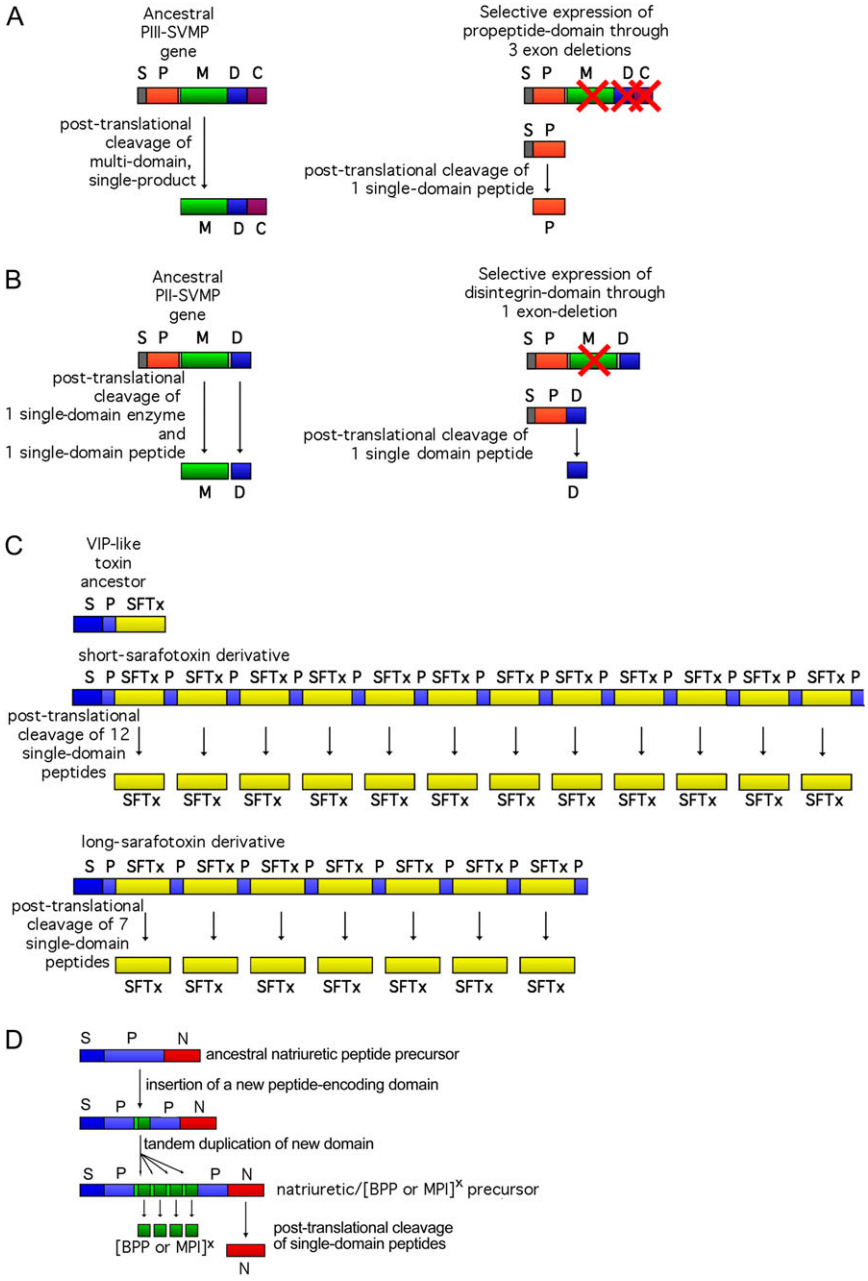

Fig. 1. *A*) P-III SVMP domain mutation producing the selective expression of the propeptide domain in *Psammophis mossambicus* snake venom. (*B*) P-II SVMP domain mutation producing the selective expression of the disintegrin domain in Viperidae snake venoms. (*C*) Tandem domain multiplication with posttranslational proteolysis of the multidomain product to liberate the sarafotoxins. (*D*) Domain mutation producing the tandemly repeated (BPPs in pit vipers or metalloprotease-inhibiting peptides [MPIs] in the *Echis* genus) medial to the natriuretic peptide–encoding domain and the subsequent posttranslational proteolysis of the multidomain product to liberate the discrete peptides. Abbreviations: BPPs = bradykinin potentiating peptides, C = cysteine-rich domain, D = disintegrin, M = metalloprotease, MPI = metalloprotease-inhibiting peptides, N = natriuretic, P = propeptide, S = signal peptide, and SFTx = sarafotoxin.

Ducancel et al. 1993; Hayashi et al. 2004). Two classes of sarafotoxin have been isolated and characterized: short (21 amino acid final processed form) and long (24 AA) that are tandemly repeated 12 and seven times, respectively (fig. 1C). Another, more extreme, example is the mutation of the monoproduct encoding ancestral natriuretic gene to encode for additional, novel, posttranslationally liberated peptides in viper venoms (fig. 1D): the bradykinin-potentiating peptides (BPPs) in pit-viper venoms (cf. Soares et al. 2005 and the tripeptide metalloprotese inhibitors in *Echis* venoms; Wagstaff et al. 2008).

As the venoms of *Heloderma* have received less attention than those of the more medically important venomous snakes, it remains unknown to what extent the chemical arsenal has undergone structural and functional innovation. Detailed knowledge of the molecular evolution of *Heloderma* toxins is not only crucial for understanding how the snake and helodermatid systems diverged from

their common venomous ancestor (Fry et al. 2006) but is also a prerequisite for insight into the structure, function, and composition of the ancestral Toxicofera venom system and how multiple lineages achieved evolutionary innovations. A thorough understanding of the molecular and functional diversity is also necessary in order to fully exploit the therapeutic potential of these venoms. In this study, we integrated transcriptome with proteome data to provide an in-depth investigation of the molecular evolution of *Heloderma* venom. Conspicuously, our analyses identify multiple domain selective expression strategies that resulted in the origin of novel toxin types.

Materials and Methods

cDNA Library Construction and Analysis

In order to investigate the relationship between toxins and the encoding transcripts and also facilitate molecular evolutionary analyses, a venom gland cDNA library was constructed to obtain full-length toxin-encoding transcripts from a *Heloderma suspectum cinctum* (banded Gila monster) specimen using the Qiagen RNeasy Midi Kit with subsequent selection of mRNAs using the Oligotex Midi Kit. cDNA libraries were constructed using the Clonetech Creator SMART cDNA library construction kit and transformed into one shot electrocompetent GeneHogs (Invitrogen Corporation, United States). Isolation and sequencing of inserts were conducted at the Australian Genome Research Facility, using BDTv3.1 chemistry with electrophoretic separation on an AB330xl. Three hundred and eighty-four colonies were sequenced, inserts screened for vector sequences, and those parts removed prior to analysis and identification.

Toxin sequences were identified by comparison of the translated DNA sequences with previously characterized toxins using Blast search of the Swiss-Prot/Uni-Prot protein database (http://www.expasy.org/tools/blast/). Molecular phylogenetic analyses of toxin transcripts were conducted using the translated amino acid sequences. Comparative sequences from other venomous reptiles and outgroups were obtained through Blast searching (http://www.expasy.org/tools/blast/) using representative toxin sequences. To minimize confusion, all sequences obtained in this study are referred to by their Genbank accession numbers (http://www.ncbi.nlm.nih.gov/sites/entrez?db=Nucleotide) and sequences from previous studies are referred to by their UniProt/Swiss-Prot accession numbers (http://www.expasy.org/cgi-bin/sprot-search-ful). Resultant sequence sets were aligned using the program ClustalX, followed by visual inspection for errors. When presented as sequence alignments, leader sequence shown in lowercase, prepro region underlined, cysteines highlighted in black, functional residues in bold. Data sets were analyzed using Bayesian inference implemented on MrBayes, version 3.0b4. The analysis was performed by running a minimum of 1×10^6 generations in four chains and saving every 100th tree. The log-likelihood score of each saved tree was plotted against the number of generations to establish the point at which the log-likelihood scores of the analysis reached their asymptote and the posterior probabilities for clades established by constructing a majority rule consensus tree for all trees generated after the completion of the burn-in phase. Sequence alignments can be obtained by emailing Dr Bryan Grieg Fry (bgf@unimelb.edu.au).

Bioactivity Characterization of Exendin, Helokinestatin, and Natriuretic Peptides

Peptide Isolation and Synthesis. In order to investigate structure–function relationships, we isolated and characterized or synthesized variants of exendin, helokinestatin, and natriuretic peptides. Following the recent discovery of Helokinestatin-1 (Kwok et al. 2008), in this study two, more isoforms were isolated and characterized from the same *H. horridum* and *H. suspectum* venom stocks used in the previous study. Thirty-five milligrams of venom (dry weight) was reconstituted in 3 ml of 2 M acetic acid, clarified by centrifugation, and applied directly to a 90-cm × 1.6-cm column of Sephadex G-50 (fine) column calibrated with Blue Dextran (V_0) and potassium dichromate (V_t), equilibrated in 2 M acetic acid and eluted at a flow rate of 10 ml/h. Fractions (2.5 ml) were collected at 15-min intervals. Gel permeation chromatographic fractions 55–65, (500 μl of each fraction) were pooled and subjected to reversedphase high-performance liquid chromatography (HPLC) fractionation using a Thermoquest gradient HPLC system fitted with a Jupiter semipreparative C-5 column (30 cm × 1 cm). This was eluted with a linear gradient formed from 0.05/99.5 (v/v) triflouroacetic acid (TFA)/water to 0.05/19.95/80.0 (v/v/v) TFA/water/acetonitrile (ACN) in 240 min at a flow rate of 1 ml/min. Fractions (1 ml) were collected at minute intervals, and the effluent absorbance was continuously monitored at λ_{214} nm. Samples (100 μl) were removed from each fraction in triplicate, lyophilized, and stored at −20 °C prior to smooth muscle pharmacological analysis. Isolated peptides were analyzed using matrix-assisted laser desorption/ionization, time-of-flight mass spectrometry (MALDI–TOF MS) on a linear time-of-flight Voyager DE mass spectrometer (Perseptive Biosystems, MA, United States in positive detection mode using alpha-cyano-4-hydroxycinnamic acid as the matrix. Internal mass calibration of the instrument with known standards established the accuracy of mass determination as ±0.1%. After determination of sample purity and molecular mass, the peptide was subjected to MS/MS fragmentation and de novo sequence analysis using a Q-TOF Ultima mass spectrometer (Micromass, Manchester, United Kingdom) and was subjected to conventional amino acid sequence analysis by automated Edman degradation using an Applied Biosystems 491 Procise microsequencer with pulsed-liquid chemistry. The limit for detection using this system was 0.2 pmol.

Helokinestatin and natriuretic peptide sequences in this study and the previously reported exendin peptides 1–4 (Swiss-Prot/Uni-Prot accession numbers P04203, P04204, P20394, and P26349) were synthesized on a CEM Liberty peptide synthesizer using Fmoc solid-phase peptide

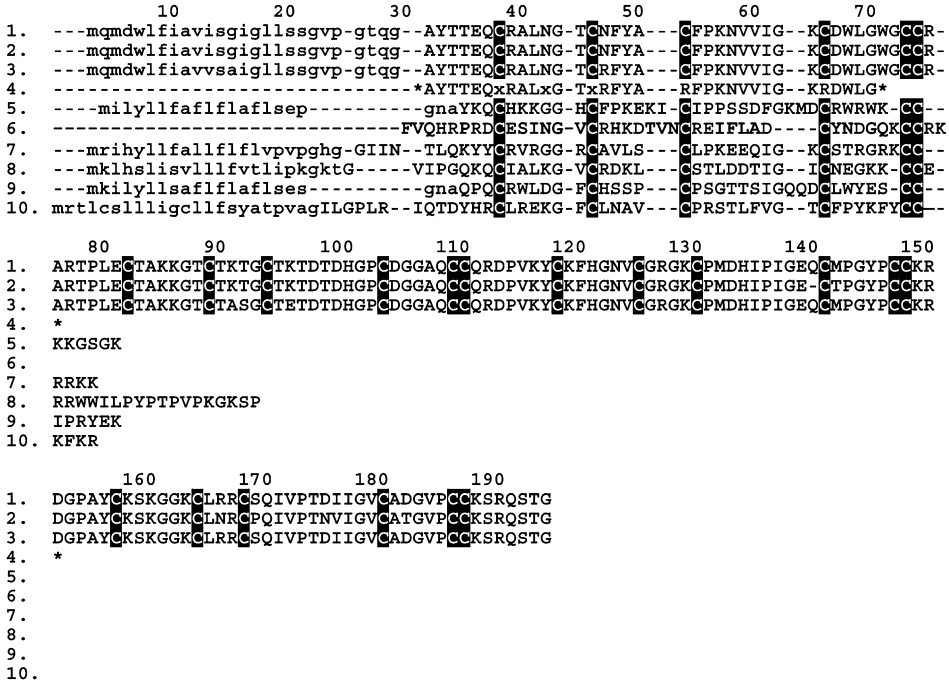

Fig. 2. Sequence alignment of the helofensin isoforms from the *Heloderma suspectum cinctum* (1. GQ918270, 2. GQ918271, and 3. EU790964). The protein fragment Q7LZ31 from *Heloderma horridum horridum* venom, representative beta-defensins convergently found in other venoms (5. O73799 *Crotalus durissus terrificus* and 7. P82172 *Ornithorhynchus anatinus*), and representative nonvenom beta-defensins (8. P81534 *Homo sapiens*, 9. Q30KJ9 *Pan troglodytes*, 10. Q6HAA2 *C. d. terrificus*, and 11. Q32ZI5 *Rattus norvegicus*). Signal peptides are shown in lowercase. * designates N-terminal fragment.

chemistry. The peptides were cleaved from the solid-phase resin with TFA/H_2O/triisopropylsilane/3,6-dioxa-1,8-octanedithiol (90:2.5:2.5:5) for 2 h. The crude peptides were isolated by ether precipitation, dissolved in 30/70, v/v, ACN/H_2O, and lyophilized. The crude linear peptides were reversed-phase HPLC purified (Agilent 1200 HPLC System) before forming the single disulfide-bond (in the natriuretic peptide only) by treatment with dipyridyldithiol (1 equiv) in 100 mM ammonium acetate (peptide concentration 1mg/ml, 30 min). The pure cyclized natriuretic peptide was isolated by directly applying the ammonium acetate solution to a reversed-phase HPLC column, isolating pure peptide fractions and lyophilization of the products. The identity of the pure cyclized peptide was confirmed by high-resolution mass spectrometry on an Agilent QTOF 6510 LC/MS mass spectrometer.

Anesthetized Rat Studies. Male Sprague–Dawley rats were anesthetized with pentobarbitone sodium (60–100 mg/kg; i.p.). A midline incision was made in the cervical region and cannulae inserted into the trachea, jugular vein, and carotid artery, for artificial respiration (if required), administration of peptides and measurement of blood pressure, respectively. Arterial blood pressure was recorded using a Gould P23 pressure transducer connected to a PowerLab system. All results were expressed as change in mean arterial pressure (MAP).

Guinea-Pig Isolated Ileum Studies. Guinea pigs of either sex were killed by CO_2 inhalation and exsanguination. The ileum was removed and cut into 2-cm segments. Segments of ileum were then mounted on wire tissue holders under 1-g resting tension in 5-ml organ baths containing physiological salt solution of the following composition (in mM): NaCl 118.4; KCl 4.7; $MgSO_4$ 1.2; KH_2PO_4 1.2; $NaHCO_3$ 25.0; glucose 11.1; and $CaCl_2$ 2.5, continuously bubbled with carbogen (95% O_2; 5% CO_2) and maintained at 34 °C. The preparation was allowed to equilibrate for 30 min. A cumulative concentration–response curve to bradykinin (1 nM–1 μM) using half-log unit increments was then obtained. The peptide (0.1 μM) was then added and left to equilibrate for 30 min. A cumulative concentration–response curve to bradykinin (1 nM–1 μM) was then repeated, in the presence of the peptide, as described above. Isometric contractions were measured via a Grass force–displacement transducer (FT03) and recorded using a Powerlab system. Responses to bradykinin in the presence of the peptide were expressed as a % of the maximum response obtained from the initial bradykinin curve.

Rat isolated Aorta. Male Sprague–Dawley rats were killed by CO_2 inhalation and exsanguination. The thoracic aorta was removed, cleaned of surrounding connective tissue, and cut into 5-mm rings. Aortic rings were mounted in organ baths containing physiological solution (as above). The aortic rings were maintained at 37 °C and suspended between wire hooks at a resting tension of 10 g. Isometric contractions were measured by a Grass force–displacement transducer (FT03) and recorded using a Powerlab. Tissues were precontracted with phenylephrine (10 μM) and, at the plateau of contraction, relaxation responses to peptides obtained.

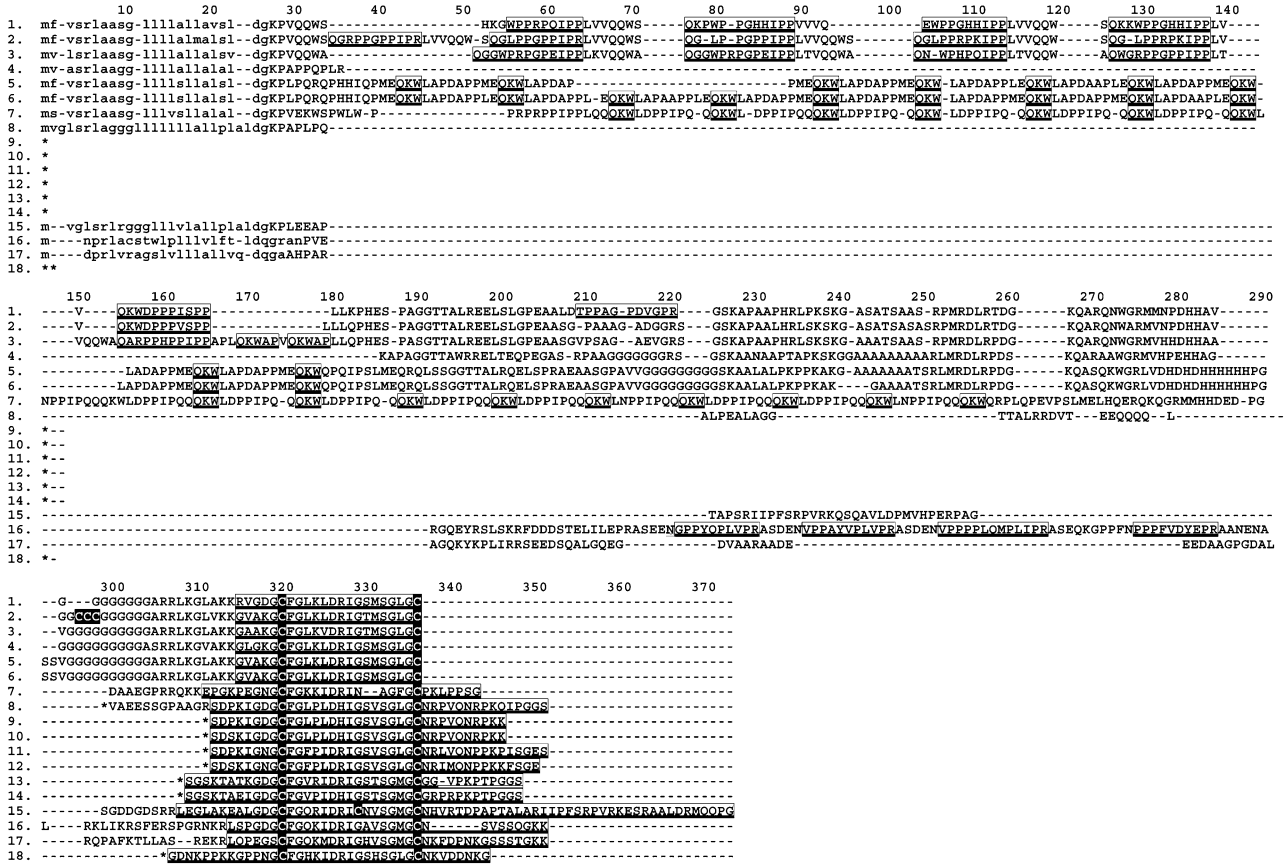

Fig. 3. Sequence alignment of Toxicofera natriuretic toxins: Q27J49 (*Lachesis muta*); 2. Q9PT52 (*Gloydius halys*); 3. Q9PW56 (*Bothrops_jararaca*); 4. Q09GK2 (*Philodryas_olfersii*); 5. A8YPR7 (*Echis_occelatus*); 6. A8YPR8 (*E. occelatus*); 7. A8YPS0 (*Cerastes cerastes*); 8. Q4VRI2 (*Oxyuranus scutellatus scutellatus*); 9. P83227 (*Oxyuranus microlepidotus*); 10. P83224 (*O. microlepidotus*); 11. Q3SAF5 (*Pseudechis australis*); 12. P83230 (*O. microlepidotus*); 13. Q1ZYW0 (*Rhinoplocephalus nigrescens*); 14. Q3SAF3 (*P. australis*); 15. P79799 (*Micrurus corallinus*); 16. EU790965 (*Heloderma suspectum cinctum*); 17. Q2XXL8 (*Varanus varius*); and 18. Q7LZ09 (*Macrovipera lebetina*). Signal peptides are shown in lowercase. Posttranslationally processed functional peptides are shown in boxes (helokinestatin in *H. suspectum*, BPPs in the viperid snake venoms; the antiplatelet peptide in 18 is underlined).

Results

Novel Toxin Isoforms and Precursors in the Helodemma Venom Transcriptome

cDNA clones were found that covered the entire precursor sequences of orthologs of the short lethal toxin-1 fragment (Q7LZ31) previously isolated from the venom of *Heloderma horridum Horridum* (Komori et al. 1988), showing it to be constructed of beta-defensin domain repeats (fig. 2), with us thus giving this class of toxins the name "helofensins." Molecular weights (kDa) and calculated p*I*s for the three isoforms were 16.884/8.65 (EU790964), 17.815/8.78 (GQ918270), and 16.795/8.84 (GQ918271). Another domain modification identified was that five peptide toxins (natriuretic peptide plus four helokinestatins) are encoded by a single mRNA transcript evolved from the monodomain natriuretic ancestral sequence (fig. 3). One helokinestatin peptide (helokinestatin-1) was previously purified from the venom (Kwok et al. 2008), and the others were purified from the venom in this study, thus allowing for determination of posttranslational cleavage sites in the translated form of the full-length mRNA transcript also recovered in this study. The first three helokinestatin isoforms were similar in sequence (GPPYQPLVPR, VPPAYVPLVPR, and VPPPPLQMPLIPR, respectively) and separated by a conserved ASDEN linker sequence (fig. 3). A linker sequence ASEQKGPPFN separates a fourth bioactive helokinestatin variant (PPPFVDYEPR), which has only one proline bracket rather than the two brackets characteristic of the other three peptides. In addition, we found a novel precursor transcript that encodes a closely related isoform of exendin 2. Despite the considerable difference in sequence and activity, this precursor sequence of the exendin 2 isoform obtained here shows overall high structural similarity to the precursors of exendins 3 and 4 (fig. 4). This is especially the case for the signal peptide, which differs in only 3 amino acids (14.3%) from that of exendin 3. For exendins, our analyses recover all known toxins and precursors in a single clade within the glucagon/vasoactive intestinal peptide (VIP)/pituitary adenylate cyclase-activating polypeptide (PACAP) protein family (fig. 5).

Bioactivity Testing

The exendin toxins were shown to have variable degrees of cardioactivity (fig. 6*A* and *B*), with exendins 1 and 2 being

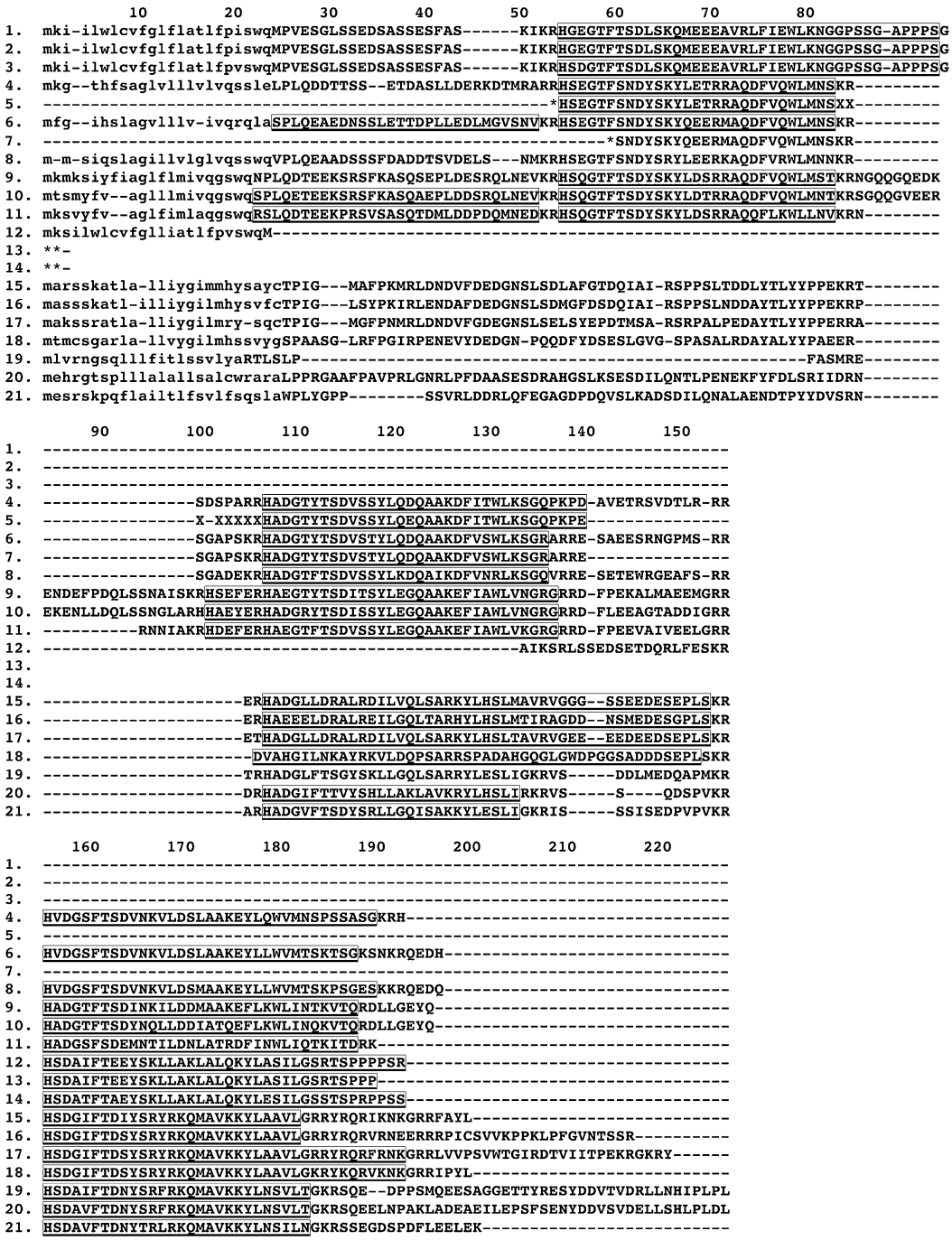

Fig. 4. Sequence alignment of exendin toxins and related nontoxins: 1. EU790959 (*Heloderma suspectum cinctum*); 2. P26349 (*H. suspectum* ssp.); 3. P20394 (*Heloderma horridum* ssp.); 4. Q6RYB9 (*Ictalurus punctatus*); 5. P04093 (*I. punctatus*); 6. Q91971 (*Oncorhynchus mykiss*); 7. Q788W6 (*Oncorhynchus tschawyts*); 8. Q6RYC2 (*Sebastes caurinus*); 9. Q3HLJ1 (*Meleagris gallopavo*); 10. O12956 (*H. suspectum* ssp.); 11. P05110 (*Cavia porcellus*); 12. EU790960 (*H. s. cinctum*); 13. P04204 (*H. suspectum* ssp.); 14. P04203 (*H. suspectum* ssp.); 15. A5YVW6 (*Ctenopharyngodon idella*); 16. A9QLJ1 (*Trichogaster trichopter*); 17. P48144 (*Clarias macrocephalus*); 18. Q29W19 (*Bos taurus*); 19. B0LF70 (*Danio rerio*); 20. P45644 (*M. gallopavo*); and 21. P01283 (*Rattus norvegicus*). Signal peptides are shown in lowercase. Posttranslationally processed functional peptides are shown in boxes. Designates incomplete N-terminal sequence. * designates incomplete N-terminal sequence.

more similar to each other and more potent than exendins 3 and 4 (which were also similar to each other) or the *Heloderma* body peptide GLP-1 (which was slightly more active than exendins 3 and 4). Reflective of significant sequence differences among the four helokinestatin peptides, helokinestatins-2, -3, and -4 were less potent than helokinestatin-1 at inhibiting contractile responses to bradykinin in the guinea-pig ileum and showed similar variable antagonist activity at bradykinin B2 receptors, with helokinestatin-1 again being the most potent (fig. 6C).

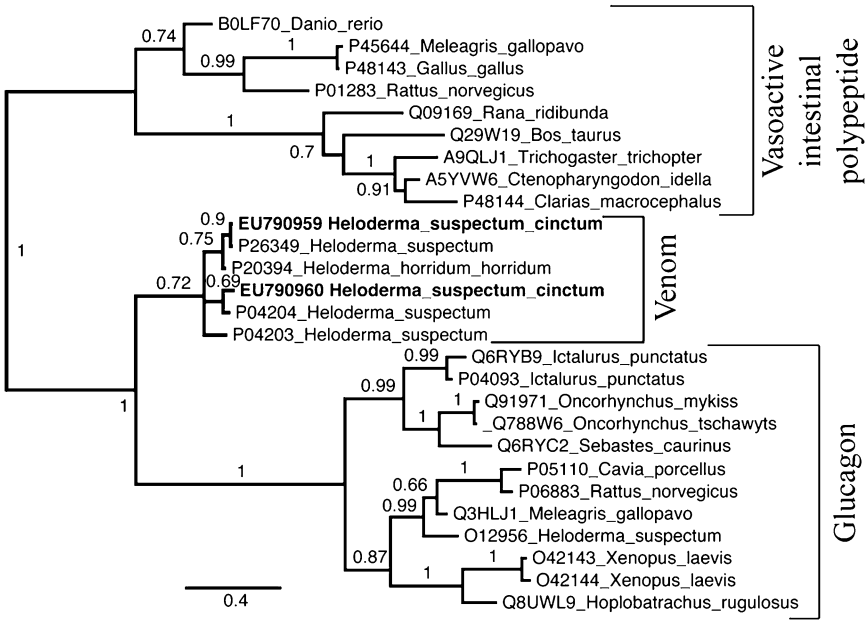

FIG. 5. Bayesian phylogenetic reconstruction of exendin toxins and related nontoxin sequences.

Discussion

Transcriptome analysis by random clone sequencing of cDNA libraries has been proven an effective way of identifying novel isoforms of previously reported toxins, as well as toxins of new protein classes (cf. Junqueira-de-Azevedo and Ho 2002; Fry et al. 2006, 2008; Wagstaff and Harrison 2006). The availability of entire cDNA precursor sequences rather than just the processed protein forms allows for largely improved phylogenetic analyses. This provides new insights into the molecular evolutionary origins of the individual *Heloderma* toxin types. Our results thus allowed us to elucidate unique domain-expression processes utilized to generate novel toxin forms.

Novel Toxin Types Produced through Gene Domain Mutation

Helofensins. This class was previously known only from a short fragment (Q7LZ31) which, due to its small size

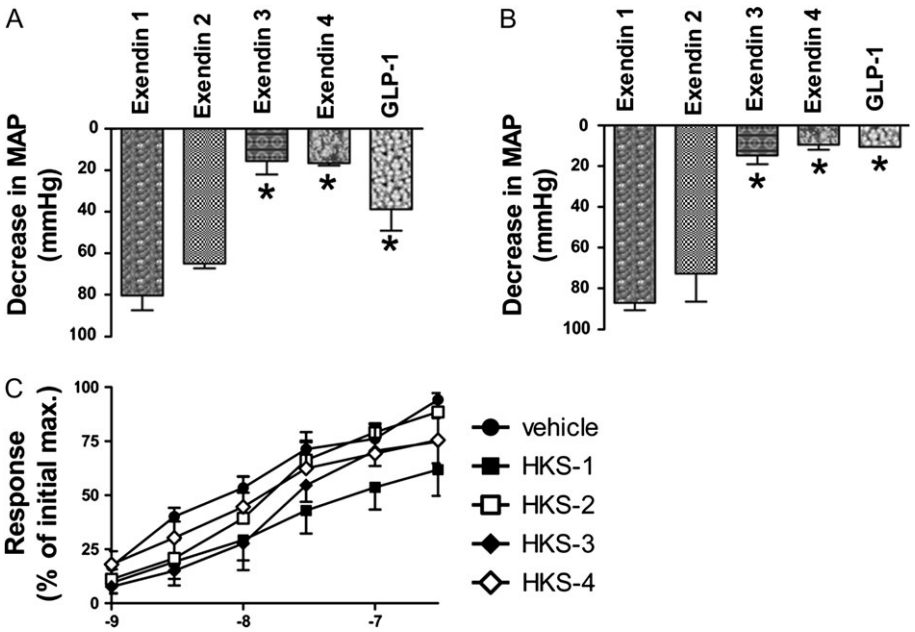

FIG. 6. *A*). Effect of exendins 1–4 or GLP-1 (100 μg/kg, i.v., $n = 3$) on the MAP of anesthetized rats. *$P < 0.05$, significantly different from exendin 1, one-way analysis of variance (ANOVA). (*B*) Effect of exendins 1–4 or GLP-1 (10 μg/ml, $n = 3$) on phenylephrine precontracted aorta. *$P < 0.05$, significantly different from exendin 1, one-way ANOVA. (*C*) Effect of helokinestatin peptides (0.1 μM; $n = 5$) on cumulative concentration–response curves to bradykinin (1 nM–0.3 μM).

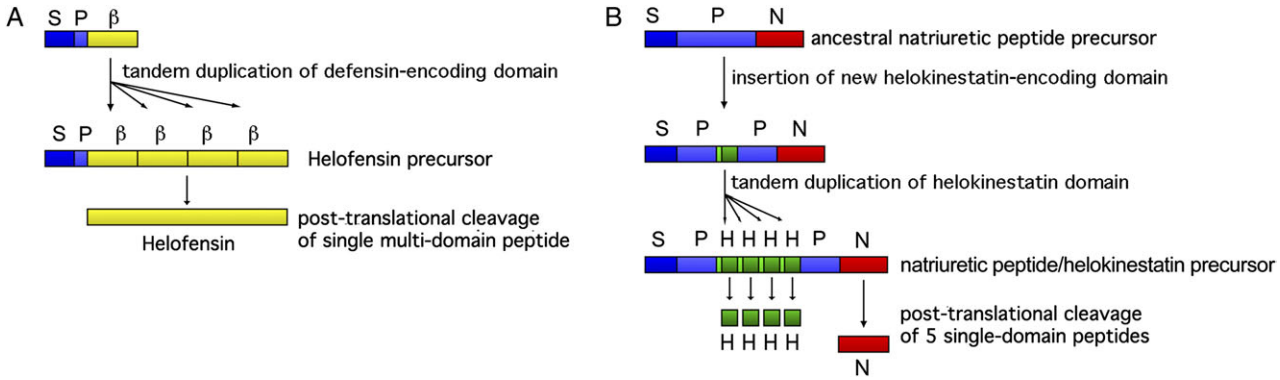

Fig. 7. *A*) Domain mutation producing the monoproduct constructed of four tandem beta-defensin domains in helofensin isoforms. (*B*) Domain mutation producing the four tandem helokinestatin peptides medial to the natriuretic peptide–encoding domain and the subsequent posttranslational proteolysis to liberate the discrete peptides. Abbreviations: β = beta-defensin, H = helokinestatin, N = natriuretic, P = propeptide, and S = signal peptide.

and sequence ambiguity for certain residues, did not permit meaningful homology searches. The 24 cysteine full-length precursor sequence of the isoforms obtained here resolves previously ambiguous residues (marked with x in fig. 2) as either cysteines (x1 and x3 being cysteines one and two, respectively) or asparagine (x2). Furthermore, two additional residues previously reported as arginine are identified here as cysteines three and four, respectively. The corresponding region of one of our sequences (EU790964) did not differ otherwise with the Q7LZ31 fragment. However, it must be noted that the calculated molecular weight of our isoforms are in conflict with the reported 28-kDA proteins in previous studies using gel-based molecular weight determination (Komori et al. 1988).

Our Blast searches and phylogenetic analyses identify helofensins as being extremely derived forms of the beta-defensin gene type. Helofensin isoforms have descended from an ancestral beta-defensin precursor that underwent three domain duplications to produce a single gene encoding four tandem repeats of the original domain (fig. 7*A*). As these four tandem-repeated domains encode a single peptide, this almost certainly results in a new and more complex protein fold. Each of these domains has subsequently undergone significant molecular evolution with changes in cysteine spacing and pattern as well as fundamental biochemical changes such as charge distribution. The cysteine pattern and spacing of the four repeats are conserved: C(6)C(4)C(9)C(6)CC, C(6)C(4)C(9)C(5)CC, C(6)C(4)C(10)C(5)CC, and C(6)C(3)C(11)C(5)CC (fig. 2). Only one residue deletion occurs between the four sequences. Charged residues were also highly conserved between the isoforms, with only one of the six residue changes (at alignment position 97) being a charge state reversal. As with the helokinestatin peptides (fig. 3), the tandem domain repeats are more degenerate downstream. These polarities of mutations in repeats suggest that there are upstream constraints/selection to conserve repeat structure at the 5′ end. As the beta-defensin domain type utilized is different than that recruited for use in the crotamine toxin multigene family (e.g., O57540), this represents a third utilization of this domain for use as a toxin, with the platypus toxin being the other distinct type (e.g., P82172).

Natriuretic Peptides. The ancestral monodomain natriuretic gene was mutated to additionally encode medially for four versions of helokinestatin peptides (fig. 3), with the five peptides liberated from each other by posttranslational proteolysis (fig. 7*B*). Such novel domains are absent from the homologous natriuretic peptides found in varanids (Fry et al. 2006, 2009), but it remains to be determined whether they are present in the forms of the more closely related anguiid lizards. The helodermatid lizards have thus convergently evolved trandemly repeated proline-rich bioactive peptides (the helokinestatin peptides) in the same upstream region of the natriuretic gene (between the signal peptide and the natriuretic peptide–encoding domain) as has occurred with the (also posttranslationally liberated) BPPs in pit-viper venoms (cf. Soares et al. 2005) and metalloprotease-inhibiting peptides in the *Echis* genus of true vipers (Wagstaff et al. 2008) (fig. 3).

Exendin Peptides. Exendin toxins pose a fascinating molecular evolutionary riddle. Although exendins 1 and 2 are similar to the second domain of the VIP precursor (corresponding to the VIP peptide itself), exendins 3 and 4 are structurally related to either the first or third domain of the glucagon precursor (fig. 4). In contrast, the strong similarity of the signal peptides and the prepro region of the two pairs of exendin-toxin types is indicative of a shared evolutionary history, pointing toward a common origin by a mono recruitment event. We propose three alternative evolutionary scenarios to explain the observed pattern conflict, each involving different genetic mechanisms.

A first scenario, unlikely in light of our phylogenetic results (fig. 5), involves an independent phylogenetic origin for each of the exendin types (fig. 8*A*). One pair of exendins (exendins 1 and 2) descending from a single toxin gene that duplicated from a VIP/PACAP-like precursor gene, whereas the second pair (exendins 3 and 4) descending from the glucagon-like precursor gene. Because both pairs represent

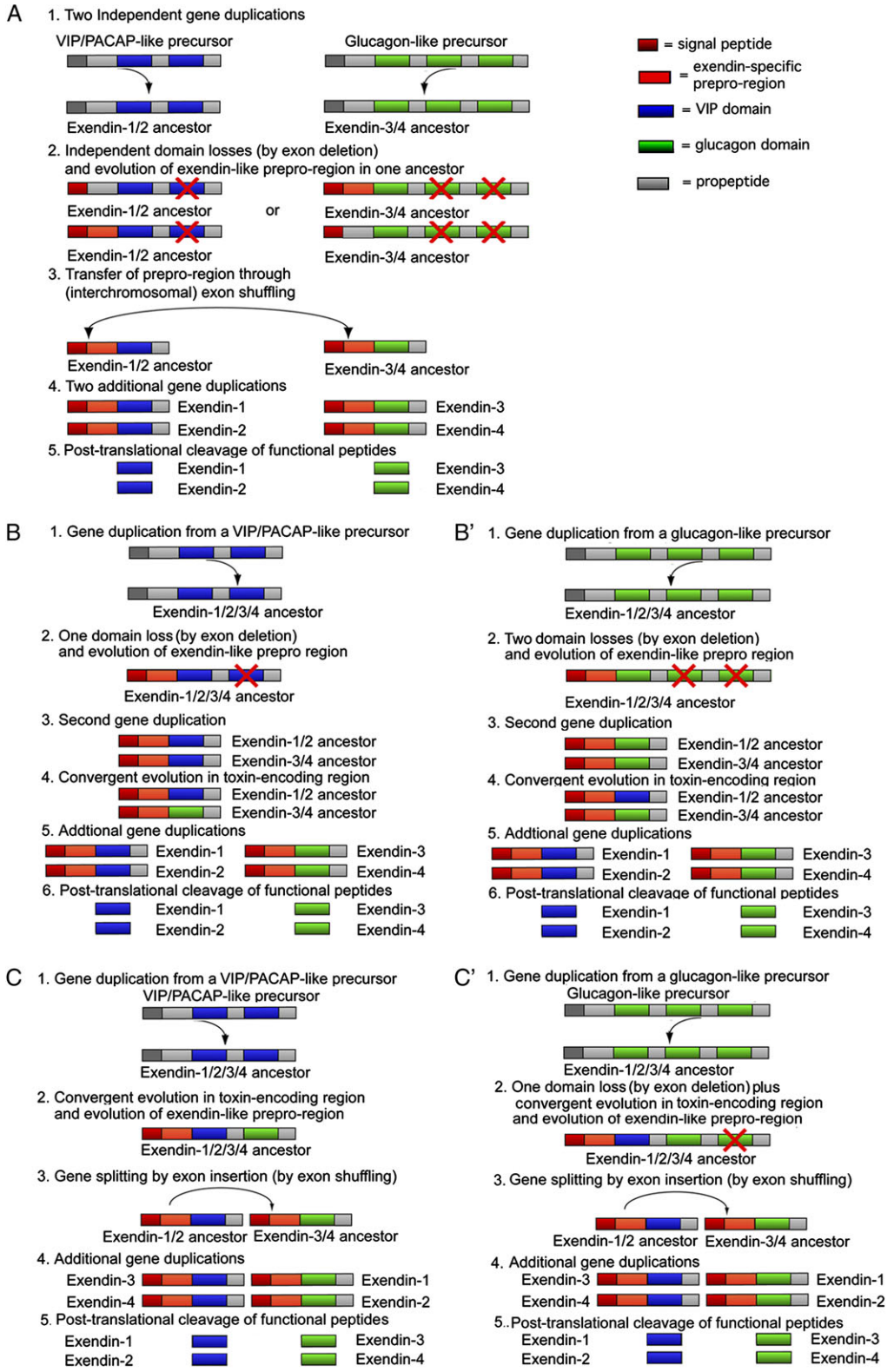

Fig. 8. Three evolutionary scenarios explaining the origin of the two monodomain exendin toxin pairs (exendins 1 and 2, and exendins 3 and 4) in *Heloderma* venoms starting from either a VIP or glucagon gene. (*A*) Ancestors of the two exendin pairs may have independently duplicated from separate ancestral multidomain hormone precursor genes. This scenario implies independent domain losses, and an exon-shuffling event to explain the closely related signal peptides among the two pairs and is unlikely in light of our phylogenetic results favoring a mono origin of exendin peptides. (*B*) A second scenario implies a monoexendin ancestor that duplicated from an unknown multidomain hormone precursor gene. The monoexendin ancestor subsequently underwent domain loss, and multiple successive gene duplication events to obtain four monodomain exendin genes. (*C*) Alternatively, an unknown multidomain ancestor was split into two tandem genes by interdomain insertion of a signal peptide through exon shuffling, and each tandem gene subsequently underwent an additional gene duplication to obtain the four exendin genes.

truncated (monodomain) precursors while all known hormone precursors in this protein family have multiple domains (VIP/PACAP precursors typically contain two domains; glucagons precursors typically have three), this implies that their respective ancestral genes independently lost one and two domain-encoding exons, respectively, to obtain their monodomain-encoding genes. In addition, dual origins would imply that the nearly identical signal peptides shared by all the exending peptides resulted from an exon-shuffling event, that is, the transfer of the signal peptide-encoding exon from one ancestral exendin to that of the other, followed by another duplication round for each exendin type. The most common mechanisms currently implicated to explain exon shuffling in eukaryotes are interlocus gene conversion (nonreciprocal recombination) and retrotransposition. Recent studies have suggested that interlocus gene conversion is most common between linked loci (on the same chromosome), and its frequency is inversely proportional to the distance between the involved loci (Ezawa et al. 2006). However, if the two pairs of exendin evolved independently from VIP and glucagon ancestors, it is unlikely that they are spatially linked. Screening of the genome maps of various vertebrates reveals that the glucagon and VIP genes are situated on different chromosomes in zebra fish (chromosomes 22 and 13, respectively), chicken (chromosomes 7 and 3), rat (chromosomes 3 and 1), and human (chromosomes 2 and 6), suggesting an ancient genomic separation of the two genes. This would imply that the VIP and glucagon genes (and any recently derived paralogs) are likely to lie on different chromosomes in *Heloderma* as well. An exon shuffling origin for the exendin signal peptides would therefore imply an interchromosomal (ectopic) gene-conversion event or a retrotransposition event. In summary, a dual origin of the two exendin gene pairs would not only imply two independent toxin recruitment events and subsequent domain losses but also an extremely rare interchromosomal exon-shuffling event.

A second scenario implicates a single evolutionary origin of exendins, as suggested by our phylogenetic analyses, with the sole founding gene either VIP (fig. 8*B*) or glucagon derived (fig. 8*B*′). Under this scenario, a single ancestral multidomain precursor gene lost one (VIP as the starting material) or two domains (glucagon as the starting material) through exon deletion(s). The structural similarities of the two exendin pairs with different hormone peptides suggest substantial convergent evolution within the peptide-encoding regions to explain their present structural variation. The timing of this would be best explained as occurring to one duplicate after the first gene duplication round subsequent to the toxin recruitment event, with another round of gene duplication producing the two exendin pairs

The third scenario, like scenario two, also implicates a single origin of exendins, again consistent with our phylogenetic analyses. This scenario involves a different type of domain mutation to explain the currently observed peptide variation, again with the sole founding gene either VIP (fig. 8*C*) or glucagon derived (fig. 8*C*′). Under these scenarios, the single ancestral multidomain precursor gene was split into two tandem genes by insertion of its signal peptide in between two of the peptide-encoding domains through exon shuffling (e.g., as a result of unequal crossing-over). The two tandem genes subsequently duplicated again, each giving rise to one of the presently observed exendin pairs. This scenario as well requires substantial convergent amino acid substitutions to explain their similarities with different hormones, with the timing occurring either just before or just after the gene splitting but before the first gene duplication round subsequent to the toxin recruitment event. This scenario would also require an exon deletion if glucagon is the starting material (fig. 8*C*′).

The first scenario is excluded by our phylogenetic analyses and also the unlikeliness of interchromosomal exon shuffling. However, the final distinction between the second and third scenarios will require insights into the genomic organization of exendins and their closely related glucagon family genes. Regardless, both the second and third scenarios would require that the ancestor of at least one of the two exendin pairs underwent substantial convergent evolution with either of the hormone clades to obtain their present structural variation. Endogenous VIP hormones have been shown to be more potent vasodilators than endogenous glucagon hormones (Ezawa et al. 2006). As a consequence, a peptide that mimics a generalized VIP hormone may provide a more effective toxin. The results of this study demonstrate that exendins 1 and 2 have a higher cardioactivity than exendins 3 and 4 and also the nontoxin peptide GLP-1 (O12956) (fig. 6*A* and *B*). This is in agreement with other studies on exendins 1 and 2 that demonstrated vasodilatory actions similar to VIP (Uddman et al. 1999; Tsueshita et al. 2004). The molecular evolution from a less potent (glucagon-like) form toward a more potent (VIP-like) form is more plausible than the converse. The origin of exendin peptides thus favors a glucagon-like ancestor with subsequent divergence of one duplicate to convergently become a VIP-like toxin (fig. 8*B*′ or *C*′). The timing of these molecular evolutionary events however remains to be resolved. Glucagon-like exendins 3 and 4 have been isolated from both *H. suspectum* and *H. horridum*, whereas the VIP-like 1 and 2 have only been isolated from *H. suspectum*. This would thus favor a basal glucagon-derived exendin type as shown in figure 8*B*′ with a subsequent VIP-like convergence specific to *H. suspectum*. However, the absence of evidence is not necessarily evidence of absence. Thus, exhaustive sequencing of the *H. horridum* venom transcriptome must be undertaken before the concluded absence of the VIP-like exendins 1 and 2 peptides can be considered as adequately supported. If exendins 1 and 2 peptides are in fact present in the venom of *H. horridum*, this would still support a glucagon basal peptide but would not allow for distinguishing between scenario B′ or C′ in figure 8 without genomic understanding of the toxins and their nontoxin ancestors.

Conclusion

Our precursor sequences reveal previously undetected molecular evolutionary patterns in *Heloderma* toxins that provide interesting starting points for studies focusing on the genetic mechanisms that underlie toxin diversification in any venomous taxon. Multiple toxin isoforms in *Heloderma* venom were not only attained by conventional gene duplication events but also by different forms of domain mutation. First, helofensins represent an example of a new multidomain, monoproduct gene that evolved by multiple tandem domain duplications from an ancestral monodomain gene (fig. 7*A*). Second, the gene encoding for natriuretic peptides plus four additional peptides is an example of a multidomain, multiproduct gene that emerged from an ancestral monodomain, monoproduct gene by domain insertion and subsequent domain duplications (fig. 7*B*). Finally, exendins represent an example of monodomain, monoproduct genes that either evolved by domain deletion from a multidomain, multiproduct gene, or by the splitting of the ancestral multidomain, multiproduct gene to encode for two new monodomain, monoproduct genes followed by insertion of a signal peptide through exon shuffling (fig. 8).

The findings of the present study combined with the information available from the literature (Beaman et al. 2006) reveal how little we still know about the toxinology of the enigmatic *Heloderma* lizards. With respect to their venoms, we do not know enough of composition, role of individual venom components in prey capture, or in vitro activities relative to subsequent physiological sequelae following envenomation. We would also like to emphasize that these species belong to an ever-growing group of threatened species that may affect biodiversity and cause an important loss of genetic information. We, therefore, hope that this study will not only stimulate further research and provide a new understanding and realization of conservation efforts but will also encourage the utilization of this precious natural resource in a sustainable and ethical manner.

Acknowledgments

We would like to express our deep appreciation for the constructive criticism by the two anonymous reviewers, which greatly improved the manuscript. This work was supported by grants to B.G.F. from the Australian Academy of Science, Australian French Association for Science and Technology, Australia and Pacific Science Foundation, CASS Foundation, International Human Frontiers Science Program Organisation, Netherlands Organisation for Scientific Research, University of Melbourne (Faculty of Medicine and Department of Biochemistry), and a Department of Innovation, Industry and Regional Development Victoria Fellowship. The work was also supported by Australian Research Council Grants and an Australian Government Department of Education, Science, and Training/EGIDE International Science Linkages grant to B.G.F. and J.A.N and a postdoctoral fellowship of FWO-Vlaanderen to K.R. The toxin nucleotide sequences reported in this paper have been submitted to GenBank with accession numbers EU790959, EU790960, EU790964, EU790965, and GQ918270, GQ918271.

References

Beaman KR, Beck DD, McGurty BM. 2006. The beaded lizard (*Heloderma horridum*) and Gila monster (*Heloderma suspectum*): a bibliography of the family Helodermatidae. *Smithsonian Herpetol Info Serv*. 136:1–66.

Beck DD. 2005. Biology of Gila monsters and beaded lizards. Berkeley (CA): University of California Press.

Bloomgren G, Braun D, Kolterman O. 2008. Exenatide and rare adverse events—reply. *N Engl J Med*. 358:1971–1972.

Bogert CM, del Campo RM. 1956. The gila monster and its allies. The relationships, habits, and behavior of the lizards of the family Helodermatidae. *Bull Am Mus Nat History*. 109:1–238.

Bouabboud CF, Kardassakis DG. 1988. Acute myocardial-infarction following a gila monster (*Heloderma suspectum cinctum*) bite. *West J Med*. 148:577–579.

Brown DE, Carmony NB. 1999. Gila monster: facts and folklore of America's Aztec lizard. Salt Lake City (UT): University of Utah Press

Calvete JJ, Marcinkiewicz C, Monleon D, Esteve V, Celda B, Juarez P, Sanz L. 2005. Snake venom disintegrins: evolution of structure and function. *Toxicon* 45:1063–1074.

Cantrell FL. 2003. Envenomation by the Mexican beaded lizard: a case report. *J Toxicol Clin Toxicol*. 41:241–244.

Chen TB, Bjourson AJ, Orr DF, Kwok H, Rao PF, Ivanyi C, Shaw C. 2002. Unmasking venom gland transcriptomes in reptile venoms. *Anal Biochem*. 311:152–156.

Chen TB, Kwok H, Ivanyi C, Shaw C. 2006. Isolation and cloning of exendin precursor cDNAs from single samples of venom from the Mexican beaded lizard (*Heloderma horridum*) and the Gila monster (*Heloderma suspectum*). *Toxicon* 47:288–295.

Chen YQE, Drucker DJ. 1997. Tissue-specific expression of unique mRNAs that encode proglucagon-derived peptides or exendin 4 in the lizard. *J Biol Chem*. 272:4108–4115.

de la Vega RCR, Merino E, Becerril B, Possani LD. 2003. Novel interactions between K+ channels and scorpion toxins. *Trends Pharmacol Sci*. 24:222–227.

Ducancel F, Matre V, Dupont C, Lajeunesse E, Wollberg Z, Bdolah A, Kochva E, Boulain JC, Menez A. 1993. Cloning and sequence-analysis of cdnas encoding precursors of sarafotoxins—evidence for an unusual rosary-type organization. *J Biol Chem*. 268:3052–3055.

Eng J, Andrews PC, Kleinman WA, Singh L, Raufman JP. 1990. Purification and structure of exendin-3, a new pancreatic secretagogue isolated from *Heloderma horridum* venom. *J Biol Chem*. 265:20259–20262.

Eng J, Kleinman WA, Singh L, Singh G, Raufman JP. 1992. Isolation and characterization of exendin-4, an exendin-3 analog, from *Heloderma suspectum* venom—further evidence for an exendin receptor on dispersed acini from guinea-pig pancreas. *J Biol Chem*. 267:7402–7405.

Ezawa K, Oota S, Saitou N. 2006. Genome-wide search of gene conversions in duplicated genes of mouse and rat. *Mol Biol Evol*. 23:927–940.

Fox JW, Serrano SMT. 2008. Insights into and speculations about snake venom metalloproteinase (SVMP) synthesis, folding and disulfide bond formation and their contribution to venom complexity. *FEBS J*. 275:3016–3030.

Fox JW, Serrano SMT. 2009. Timeline of key events in snake venom metalloproteinase research. *J Proteom*. 72:200–209.

Fry BG. 2005. From genome to "venome": molecular origin and evolution of the snake venom proteome inferred from

phylogenetic analysis of toxin sequences and related body proteins. *Genome Res*. 15:403–420.

Fry BG, Scheib H, van der Weerd L, Young B, McNaughtan J, Ramjan SFR, Vidal N, Poelmann RE, Norman JA. 2008. Evolution of an arsenal. *Mol Cell Proteom*. 7:215–246.

Fry BG, Vidal N, Norman JA, et al. (14 co-authors). 2006. Early evolution of the venom system in lizards and snakes. *Nature* 439:584–588.

Fry BG, Wickramaratana JC, Lemme S, Beuve A, Garbers D, Hodgson WC, Alewood P. 2005. Novel natriuretic peptides from the venom of the inland taipan (*Oxyuranus microlepidotus*): isolation, chemical and biological characterisation. *Biochem Biophys Res Commun*. 327:1011–1015.

Fry BG, Wroe S, Teeuwisse W, et al. (27 co-authors). 2009. A central role for venom in predation by *Varanus komodoensis* (Komodo Dragon) and the extinct giant *Varanus (Megalania) priscus*. *Proc Natl Acad Sci USA*. 106:8969–8974.

Fry BG, Wuster W, Kini RM, Brusic V, Khan A, Venkataraman D, Rooney AP. 2003. Molecular evolution and phylogeny of elapid snake venom three-finger toxins. *J Mol Evol*. 57:110–129.

Grundemar L, Hakanson R. 1992. Unlike vip, the vip-related peptides pacap, helodermin and helospectin suppress electrically evoked contractions of rat vas-deferens. *Regul Peptides*. 40:331–337.

Hayashi MAF, Ligny-Lemaire C, Wollberg Z, et al. (12 co-authors). 2004. Long-sarafotoxins: characterization of a new family of endothelin-like peptides. *Peptides* 25:1243–1251.

Hooker KR, Caravati EM. 1994. Gila monster envenomation. *Ann Emerg Med*. 24:731–735.

Junqueira-de-Azevedo IDM, Ho PL. 2002. A survey of gene expression and diversity in the venom glands of the pitviper snake *Bothrops insularis* through the generation of expressed sequence tags (ESTs). *Gene* 299:279–291.

Komori Y, Nikai T, Sugihara H. 1988. Purification and characterization of a lethal toxin from the venom of *Heloderma horridum horridum*. *Biochem Biophys Res Commun*. 154:613–619.

Kwok HF, Chen T, O'Rourke M, Ivanyi C, Hirst D, Shaw C. 2008. Helokinestatin: a new bradykinin B-2 receptor antagonist decapeptide from lizard venom. *Peptides* 29:65–72.

Mebs D. 1969a. Purification and properties of a kinin liberating enzyme from venom of *Heloderma suspectum*. *Naunyn-Schmiedebergs Archiv Pharmakol*. 264:280.

Mebs D. 1969b. Isolation and properties of kallikrein from venom of gila monster (*Heloderma suspectum*). *Hoppe-Seylers Z Physiol Chem*. 350:821.

Mochcamorales J, Martin BM, Possani LD. 1990. Isolation and characterization of helothermine, a novel toxin from *Heloderma horridum horridum* (Mexican beaded lizard) venom. *Toxicon* 28:299–309.

Morrissette J, Kratzschmar J, Haendler B, et al. (11 co-authors). 1995. PRIMARY Structure and properties of helothermine, a peptide toxin that blocks ryanodine receptors. *Biophys J*. 68: 2280–2288.

Mouhat S, Jouirou B, Mosbah A, De Waard M, Sabatier JM. 2004. Diversity of folds in animal toxins acting on ion channels. *Biochem J*. 378:717–726.

Neidigh JW, Fesinmeyer RM, Prickett KS, Andersen NH. 2001. Exendin-4 and glucagon-like-peptide-1: NMR structural comparisons in the solution and micelle-associated states. *Biochemistry* 40:13188–13200.

Nikai T, Imai K, Sugihara H, Tu AT. 1988. Isolation and characterization of *horridum* toxin with arginine ester hydrolase activity from *Heloderma horridum* (beaded lizard) venom. *Arch Biochem Biophys*. 264:270–280.

Nobile M, Magnelli V, Lagostena L, Mochcamorales J, Possani LD, Prestipino G. 1994. The toxin helothermine affects potassium currents in newborn rat cerebellar granule cells. *J Membr Biol*. 139:49–55.

Nobile M, Noceti F, Prestipino G, Possani LD. 1996. Helothermine, a lizard venom toxin, inhibits calcium current in cerebellar granules. *Exp Brain Res*. 110:15–20.

Parker DS, Raufman JP, Odonohue TL, Bledsoe M, Yoshida H, Pisano JJ. 1984. Amino-acid-sequences of helospectins, new members of the glucagon superfamily, found in gila monster venom. *J Biol Chem*. 259:1751–1755.

Soares MR, Oliveira-Carvalho AL, Wermelinger LS, Zingali RB, Ho PL, Junqueira-de-Azevedo IDM, Diniz MRV. 2005. Identification of novel bradykinin-potentiating peptides and C-type natriuretic peptide from *Lachesis muta* venom. *Toxicon* 46:31–38.

Strimple PD, Tomassoni AJ, Otten EJ, Bahner D. 1997. Report on envenomation by a Gila monster (*Heloderma suspectum*) with a discussion of venom apparatus, clinical findings, and treatment. *Wild Environ Med*. 8:111–116.

Takasaki C, Tamiya N, Bdolah A, Wollberg Z, Kochva E. 1988. Sarafotoxins-s6-several isotoxins from *Atractaspis engaddensis* (burrowing asp) venom that affect the heart. *Toxicon* 26: 543–548.

Tsueshita T, Onyukusel H, Sethi V, Gandhi S, Rubinstein I. 2004. Helospectin I and II evoke vasodilation in the intact peripheral microcirculation. *Peptides* 25:65–69.

Uddman R, Goadsby PJ, Jansen-Olesen I, Edvinsson L. 1999. Helospectin-like peptides: immunochemical localization and effects on isolated cerebral arteries and on local cerebral blood flow in the cat. *J Cereb Blood Flow Metab*. 19:61–67.

Utaisincharoen P, Mackessy SP, Miller RA, Tu AT. 1993. Complete primary structure and biochemical-properties of gilatoxin, a serine-protease with kallikrein-like and angiotensin-degrading activities. *J Biol Chem*. 268:21975–21983.

Vidal N, Hedges SB. 2005. The phylogeny of squamate reptiles (lizards, snakes, and amphisbaenians) inferred from nine nuclear protein-coding genes. *C R Biol*. 328:1000–1008.

Wagstaff SC, Favreau P, Cheneval O, Laing GD, Wilkinson MC, Miller RL, Stocklin R, Harrison RA. 2008. Molecular characterisation of endogenous snake venom metalloproteinase inhibitors. *Biochem Biophys Res Commun*. 365:650–656.

Wagstaff SC, Harrison RA. 2006. Venom gland EST analysis of the saw-scaled viper, *Echis ocellatus*, reveals novel alpha(9)beta(1) integrin-binding motifs in venom metalloproteinases and a new group of putative toxins, renin-like aspartic proteases. *Gene* 377:21–32.